Macromolecules

ARTICLE

pubs.acs.org/Macromolecules

Conjugated Polymers Based on a S- and N-Containing Heteroarene: Synthesis, Characterization, and Semiconducting Properties

Yagang Chen,[†,‡] Hongkun Tian,[†] Donghang Yan,[†] Yanhou Geng,[*,†] and Fosong Wang[†]

[†]State Key Laboratory of Polymer Physics and Chemistry, Changchun Institute of Applied Chemistry, Chinese Academy of Sciences, Changchun 130022, P. R. China

[‡]Graduate School of Chinese Academy of Sciences, Beijing 100049, P. R. China

Supporting Information

ABSTRACT: Three alternating conjugated polymers (**P-bTC10**, **P-bTC12**, and **P-bTC16**) comprising a novel S- and N-containing heteroarene, i.e., *N*-dodecyldithieno[2,3-*b*;7,6-*b*]carbazole, and 4,4′-dialkyl-2,2′-bithiophenes have been designed and synthesized. The nitrogen atom in the heteroarene allows introducing an additional alkyl substituent in each repeating unit of the polymers. The resulting polymers are thermally stable with decomposition temperature of ~400 °C and highly soluble in various organic solvents, such as tetrahydrofuran (THF), toluene, chloroform, and chlorobenzene, etc. Bottom gate, top contact OTFT devices were fabricated by solution casting. Mobility of the devices increased with an increase of the alkyl chain length in bithiophene units, and **P-bTC10**, **P-bTC12**, and **P-bTC16** exhibited the mobilities up to 0.0064, 0.022, and 0.035 $cm^2/(V\ s)$, respectively. The mobility of **P-bTC16** is comparable to that of regioregular poly(3-hexylthiophene) (rr-P3HT) reference devices, indicating that this heteroarene is a potential building block for high-mobility conjugated polymers.

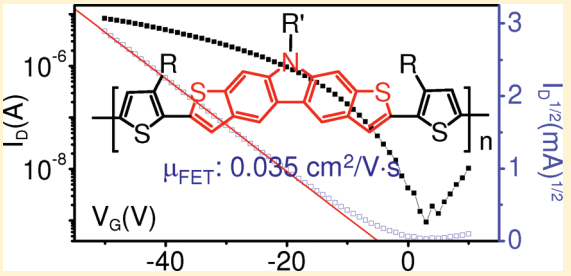

INTRODUCTION

Semiconducting polymers have attracted great attention for their applications in printable electronics.[1−4] Thiophene-containing conjugated polymers are highly promising toward aforementioned applications due to their solution processability and high field effect mobility.[5,6] Regioregular poly(3-hexylthiophene) (rr-P3HT) is the first semiconducting polymer offering mobility over 0.1 $cm^2/(V\ s)$.[7] To improve the mobility and stability, various thiophene-based conjugated polymers with strong $\pi-\pi$ interaction in the solid state and higher ionization potential have been developed by tuning alkyl chain density/length and introducing other aromatic units in polythiophene backbone.[8−24]

Some fused aromatic molecules, such as pentacene and S-containing heteroarenes,[25−29] exhibit mobility beyond 1 $cm^2/(V\ s)$ owing to their strong intermolecular $\pi-\pi$ interaction in the crystalline state. It is believed that integrating these units into conjugated polymers might render the materials high mobility.[30,31] Particularly, S-containing fused aromatics are very attractive for this purpose since they are more stable than benzene-based acenes, and the thiophene rings fused at the ends of the fused aromatics can avoid twisting between the adjacent aromatic units in the polymer backbone. With this molecular design concept, several thiophene-based conjugated polymers comprising S-containing heteroarenes have been reported.[32−35] However, with the increase of the size of the S-containing heteroarenes, density of the alkyl chains along the polymer chain decreases, which may result in the low solubility of the polymers. Meanwhile, it is known that the interaction of alkyl side chains is very important for the polymers forming highly ordered films in the solid state.[5] Low alkyl chain density may be detrimental to the self-assembly properties of the resulting polymers. In this regard, introducing more alkyl chains to the peripheries of the heteroarene units is necessary to obtain the polymers with sufficient solubility and self-assembly properties.

Carbazole is one of the most important aromatic units for designing high-performance polymers for light-emitting diodes, solar cells, and thin film transistors.[36−38] Incorporation of this unit into heteroarenes can allow introducing more alkyl chains into the polymer peripheries for improving solubility due to the presence of a nitrogen atom. With this opinion in mind, in the current paper, we designed and synthesized a new heteroarene, i.e., dithieno[2,3-*b*;7,6-*b*]carbazole, with carbazole unit in the center and thiophene rings fused at the ends. A series of conjugated polymers, i.e., **P-bTC10**, **P-bTC12**, and **P-bTC16**, as shown in Chart 1, were synthesized by Stille coupling reaction, and their properties were characterized in detail.

RESULTS AND DISCUSSION

Synthesis and Characterization. The synthesis of the heteroarene *N*-dodecyldithieno[2,3-*b*;7,6-*b*]carbazole (**4**) and polymers is outlined in Scheme 1. *N*-Dodecyl-2,7-dibromo-3,6-diiodocarbazole (**2**) was prepared by the iodination of *N*-dodecyl-2,7-dibromocarbazole (**1**) with KI/KIO_3 in acetic acid in a yield of 75%,[39] which reacted with trimethylsilylacetylene in a typical Sonogashira reaction condition to afford **3** in a yield of

Received: March 29, 2011
Revised: June 1, 2011
Published: June 15, 2011

56%. The subsequent cyclization reaction in the presence of Na_2S in *N*-methyl-2-pyrrolidone (NMP) at 190 °C yielded **4** as a white solid in a yield of 68%.[40] The organotin reagent **5** was synthesized by deprotonation with *n*-BuLi followed by quenching with trimethyltin chloride. 2,2′-Bithiophene derivatives were synthesized according to the literature procedure.[32] The polymers were synthesized by Stille coupling reaction with $Pd_2(dba)_3$/P(*o*-tol)$_3$ as catalyst in the yields of 75−84%. All polymers were purified by extraction on a Soxhlet's extractor with acetone, hexane, and chloroform in succession. The final product was obtained by precipitating the chloroform solution in methanol and dried in vacuum at room temperature. Their chemical structures were validated by ^{1}H NMR and elemental analysis. Number-average molecular weights (M_n) and polydispersity indices (PDI) are in the range of 19−22 kDa and 1.9−2.4, respectively, as measured by gel permeation chromatography (GPC) with polystyrene as standard (Table 1). All polymers are soluble in tetrahydrofuran (THF), chloroform, chlorobenzene, and *o*-dichlorobenzene. It should be pointed out that **P-bTC12** and **P-bTC16** are also soluble in toluene and xylene at room temperature, which are environmentally benign solvents for manufacture process compared to chlorinated solvents.

Chart 1. Conjugated Polymers Based on Dithieno[2,3-*b*;7,6-*b*]carbazole

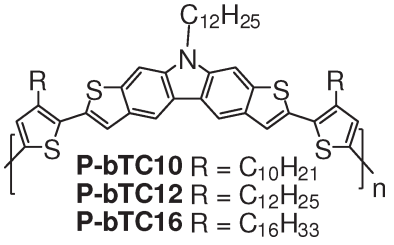

Photophysical Properties. Figure 1a shows solution absorption spectra of the polymers and heteroarene **4**. All polymers showed featureless absorption bands with the absorption maxima at 457, 454, and 450 nm for **P-bTC10**, **P-bTC12**, and **P-bTC16**, respectively. Compared with heteroarene **4**, the polymers exhibited ∼60 nm red-shifts, indicating that they are highly conjugated. A small blue-shift of the absorption maxima of the polymers was also observed from **P-bTC10** to **P-bTC12** and **P-bTC16**. This phenomenon cannot be attributed to the difference of the conjugation length since three polymers have identical chain length and conjugated backbone (the numbers of the repeating units are 21, 20, and 21 for **P-bTC10**, **P-bTC12**, and **P-bTC16**, respectively, as calculated from M_n). We postulate that this difference of the absorption maxima is originated from different aggregation capability of the polymers. It is easier to form aggregates for polymers with shorter alkyl chains. A ∼30 nm red-shift of the absorption maxima was observed for the polymers from solution to film (Figure 1b). A shoulder absorption band also appeared at ∼520 nm, indicating a more rigid and extended chain conformation of the polymers in the solid state. Compared to **P-bTC10** and **P-bTC16**, **P-bTC12** showed a 7 nm red-shift of absorption maximum along with the more obvious absorption shoulder, indicating a more extended or rigid chain conformation. Since all alkyl chains in **P-bTC12** are in the same length, this may imply that alkyl chains have noticeable effect on the backbone arrangement of the polymers in the solid state. Recently, He et al. observed an odd−even effect for conjugated polymers comprising β-alkyl-substituted fused thiophene units.[32] For the

Scheme 1. Synthetic Route of the Monomers and Polymers[a]

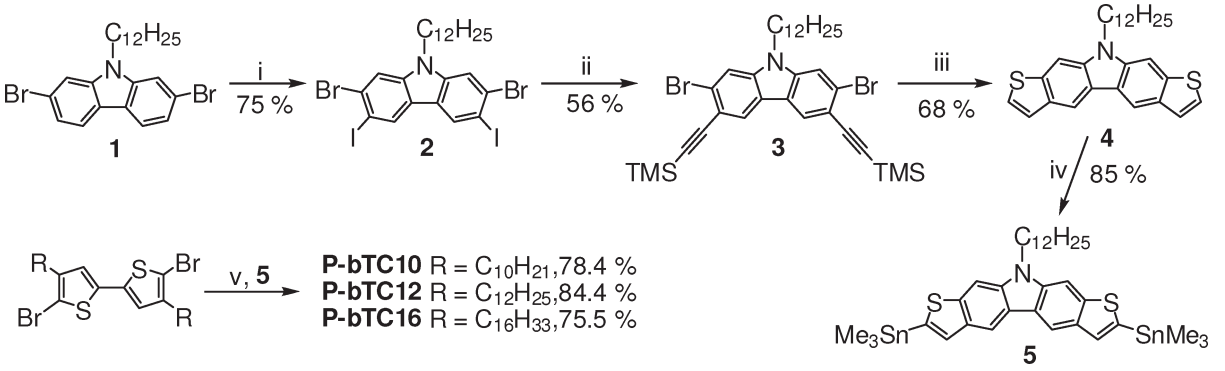

[a] Reagents and conditions: (i) KI, KIO_3, AcOH, 80 °C; (ii) trimethylsilylacetylene, $Pd(PPh_3)_2Cl_2$, CuI, Et_3N, THF, room temperature; (iii) $Na_2S·9H_2O$, NMP, 190 °C; (iv) *n*-BuLi, Me_3SnCl, THF, −20 °C to room temperature; (v) $Pd_2(dba)_3$, P(*o*-tol)$_3$, toluene, 120 °C.

Table 1. Number-Average Molecular Weights (M_n), Polydispersity Indices (PDI), and Photophysical and Electrochemical Properties of P-bTC10, P-bTC12, and P-bTC16

		λ_{abs}^{max} (nm)				
polymer	M_n (kDa)/PDI	solution[a]	film	E_g^{opt} (eV)[b]	E_{onset}^{ox} (V vs SCE)/HOMO (eV)[c]	E_{onset}^{re} (V vs SCE)/LUMO (eV)[c]
P-bTC10	1.95/2.37	457	482	2.23	0.57/−4.96	−1.87/−2.51
P-bTC12	1.86/2.14	454	489	2.22	0.55/−4.95	−1.87/−2.48
P-bTC16	2.17/1.91	450	482	2.23	0.60/−4.99	−1.88/−2.49

[a] 10^{-5} mol/L of the repeating units in chlorobenzene. [b] The optical bandgaps (E_g^{opt}) calculated from the film absorption onsets. [c] The highest occupied molecular orbital (HOMO) and the lowest unoccupied molecular orbital (LUMO) energies were calculated according to HOMO = −(4.80 + E_{onset}^{ox}) eV and LUMO = −(4.80 − E_{onset}^{re}) eV, in which E_{onset}^{ox} and E_{onset}^{re} represent oxidation onset potential and reduction onset potential, respectively.

dx.doi.org/10.1021/ma2007249 |*Macromolecules* 2011, 44, 5178–5185

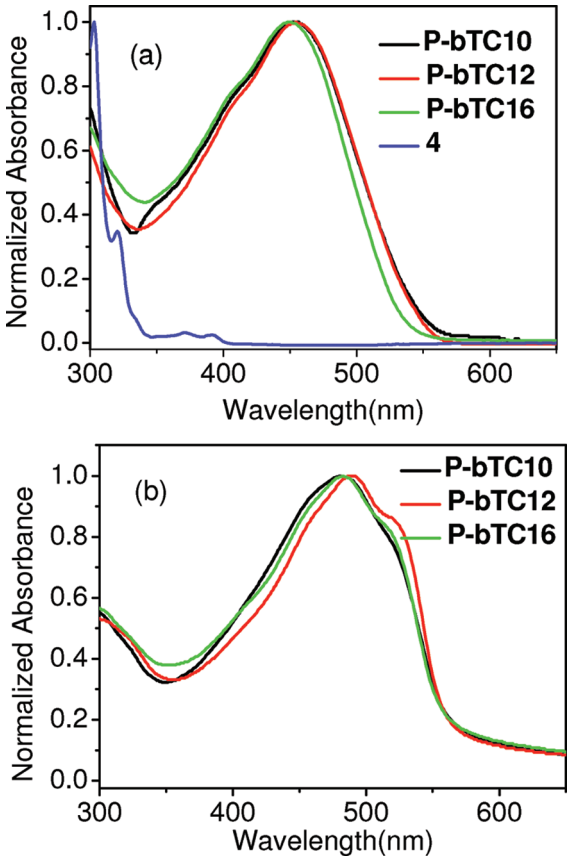

Figure 1. Solution (a) and film (b) UV−vis absorption spectra of **P-bTC10**, **P-bTC12**, and **P-bTC16**. Solution spectra were measured in chlorobenzene with a concentration of 10^{-5} mol/L. Films with a thickness of ~50 nm were prepared by spin-casting the chlorobenzene solutions with a concentration of 6.5 mg/mL on quartz substrates. Solution spectrum of **4** was also included in (a) for comparison.

polymers containing the fused thiophene units with 3 or 5 thiophene rings, only a small red-shift of absorption maxima was observed from solution to film. In contrast, the film absorption maxima of the polymer containing the fused thiophene units with 4 thiophene rings exhibited a large red-shift relative to the solution values. They contributed this difference to the effect of alkyl chain orientation on the packing of polymer backbone. Our results in the current paper indicate that increasing alkyl chain density might be able to modulate the packing behavior of polymer backbones.

Electrochemical Properties. Cyclic voltammentry (CV) was employed to study the electrochemical properties of the polymers. *N,N*-Dimethylformamide (DMF) and acetonitrile were used as the solvents for the scans in the negative and positive potential regions, respectively. CV of rr-P3HT was also measured for comparison. As shown in Figure 2 and Table 1, **P-bTC10**, **P-bTC12**, and **P-bTC16** showed identical redox behavior with similar oxidation onset potentials (E^{ox}_{onset}) at ~0.6 V and reduction onset potentials (E^{re}_{onset}) at ~−1.9 V vs SCE, respectively. The highest occupied molecular orbital (HOMO) and the lowest unoccupied molecular orbital (LUMO) levels of the polymers were estimated according to the equations HOMO = −(4.80 + E^{ox}_{onset}) eV and LUMO = −(4.80 − E^{re}_{onset}) eV.[41] As shown in Table 1, **P-bTC10**, **P-bTC12**, and **P-bTC16** exhibit HOMO levels of −4.96, −4.95, and −4.99 eV, respectively, which are

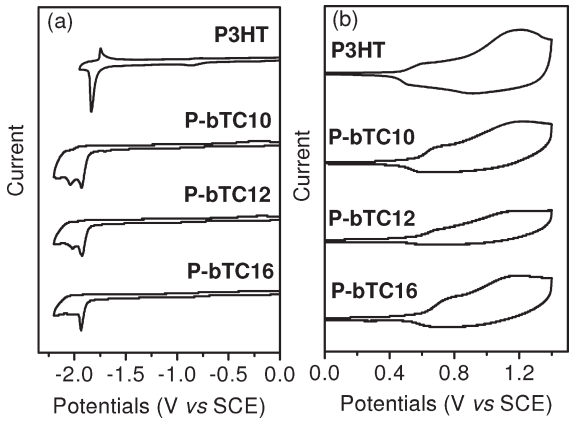

Figure 2. Thin film cyclic voltammograms (CV) of **P-bTC10**, **P-bTC12**, and **P-bTC16**. The scans in the negative (a) and positive (b) potential regions were measured in *N,N*-dimethylformamide (DMF) and acetonitrile, respectively, at a scan rate of 100 mV/s with Bu_4NPF_6 (0.1 mol/L) as electrolyte. The films of ~50 nm were prepared by spin-casting chlorobenzene solutions on the working electrode. For comparison, the film CV of rr-P3HT was also measured in the same condition.

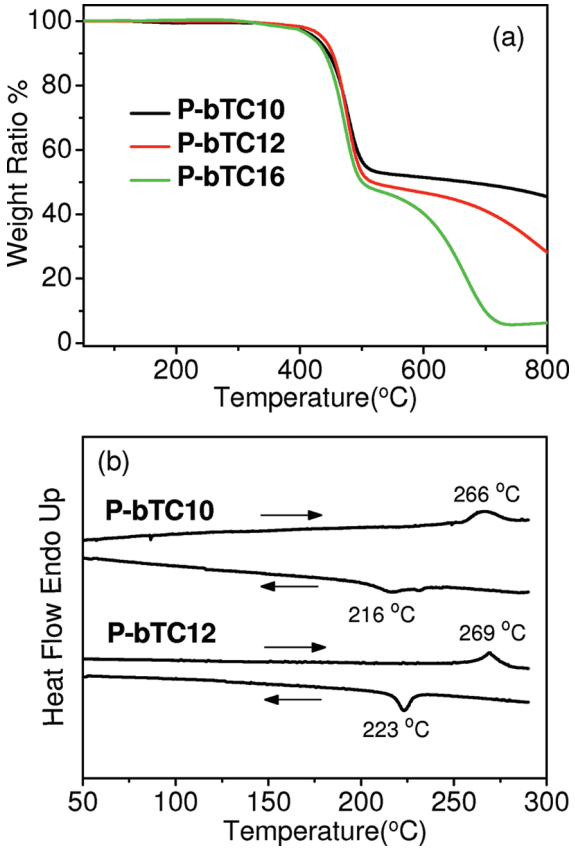

Figure 3. TGA (a) and DSC (b) curves of **P-bTC10**, **P-bTC12**, and **P-bTC16** in nitrogen with a heating/cooling rate of 10 °C/min.

about 0.1 eV lower than that of rr-P3HT (−4.89 eV). Lower HOMO levels can make these polymers more stable against oxidation than rr-P3HT.

Thermal Properties. Thermal stability was evaluated by thermogravimetric analysis (TGA) in N_2. As shown in Figure 2a, all

dx.doi.org/10.1021/ma2007249 |*Macromolecules* 2011, 44, 5178–5185

Table 2. OTFT Device Performance of P-bTC10, P-bTC12, and P-bTC16

polymer	solvent	annealing temperature	μ_{FET}^{max} ($cm^2\ V^{-1}\ s^{-1}$)[b]	μ_{FET}^{ave} ($cm^2\ V^{-1}\ s^{-1}$)[b]	V_T (V)[c]	I_{on}/I_{off}[d]
P-bTC10	CB[a]	pristine	0.0022	0.0021 ± 0.0001	−4.1 to −5.4	10^3
		180 °C	0.0064	0.0050 ± 0.0014	−6.7 to −10	10^3
P-bTC12	toluene	pristine	0.0029	0.0028 ± 0.0001	−0.21 to −1.7	10^3
		180 °C	0.0082	0.0072 ± 0.0010	1.4 to 9.0	10^4
	CB	pristine	0.0092	0.0087 ± 0.0005	3.5 to 3.8	10^3
		180 °C	0.022	0.018 ± 0.004	−2.7 to −7.2	10^4
P-bTC16	toluene	pristine	0.0071	0.0062 ± 0.0010	0.31 to 4.1	10^3
		150 °C	0.020	0.018 ± 0.002	3.5 to 6.9	10^4
	CB	pristine	0.016	0.014 ± 0.002	4.0 to 8.9	10^3
		150 °C	0.035	0.028 ± 0.007	−4.5 to −8.6	10^4

[a] CB = chlorobenzene. [b] Mobility calculated from saturation region; average mobility was calculated from 8 to 10 parallel devices. [c] Threshold voltage. [d] Current on/off ratio.

polymers are highly thermal stable with decomposition temperatures of ~400 °C. Differential scanning calorimetry (DSC) analysis was also performed in N_2 with a heating/cooling rate of 10 °C/min to observe if there are any phase transitions. As shown in Figure 2b, a phase transition at 266 °C for **P-bTC10** and 269 °C for **P-bTC12** was observed (Figure 1b), contributed to the backbone melting. No any transition was observed for **P-bTC16** below decomposition temperature, which was also found in other conjugated polymers comprising large heteroarenes.[32,33]

OTFT Performance. OTFT devices were fabricated on heavily doped n-type silicon wafers with 300 nm thermally grown SiO_2 (C_i = 10 nF cm^{-2}). The substrate surface was treated with hexamethyldisilazane (HMDS) before device fabrication according to the reference procedure.[42] The polymer layer was spin-cast on the substrate from a chlorobenzene or toluene solution. Finally, gold source and drain electrodes (40 nm) were evaporated on top through a shadow mask with a channel width (W) of 3000 μm and a channel length (L) of 100 μm. Thermal annealing of the polymer layers was also carried out for improving the film order before the deposition of the electrodes. The optimized thermal annealing temperatures are 180 °C for **P-bTC10** and **P-bTC12** and 150 °C for **P-bTC16**. The mobility was calculated from the saturation region, and the performance data are outlined in Table 2. Figure 4 shows the typical output and transfer characteristics of OTFT devices. All devices show p-type characteristics and operate in an accumulation mode. The mobilities of the devices fabricated with chlorobenzene as solvent are 2−3 times those fabricated with toluene as solvent. The device mobilities increase from **P-bTC10** to **P-bTC12** and **P-bTC16**, with the increase of the length of the alkyl substituents on bithiophene units, like the phenomenon observed in the polymers based on naphthodithiophene.[34] For instance, the devices based on the pristine and thermal-annealed films of **P-bTC10** exhibit mobilities up to 0.0022 and 0.0064 $cm^2/(V\ s)$, respectively, while those based on the pristine and thermal-annealed films of **P-bTC16** show mobilities up to 0.016 and 0.035 $cm^2/(V\ s)$, respectively. It should be pointed out that the mobility of **P-bTC16** is comparable to that of the reference devices based on rr-P3HT. (The mobility of rr-P3HT reference devices is in the range 0.03−0.04 $cm^2/(V\ s)$.) Recently, Müllen et al. and He et al. reported polymers based on S-containing heteroarenes comprising 6 and 5 fused rings, respectively. However, these polymers showed OTFT mobilities only in the level of 10^{-3} $cm^2/(V\ s)$.[32,35] Bao et al. also reported the polymers based on anthradithiophene,

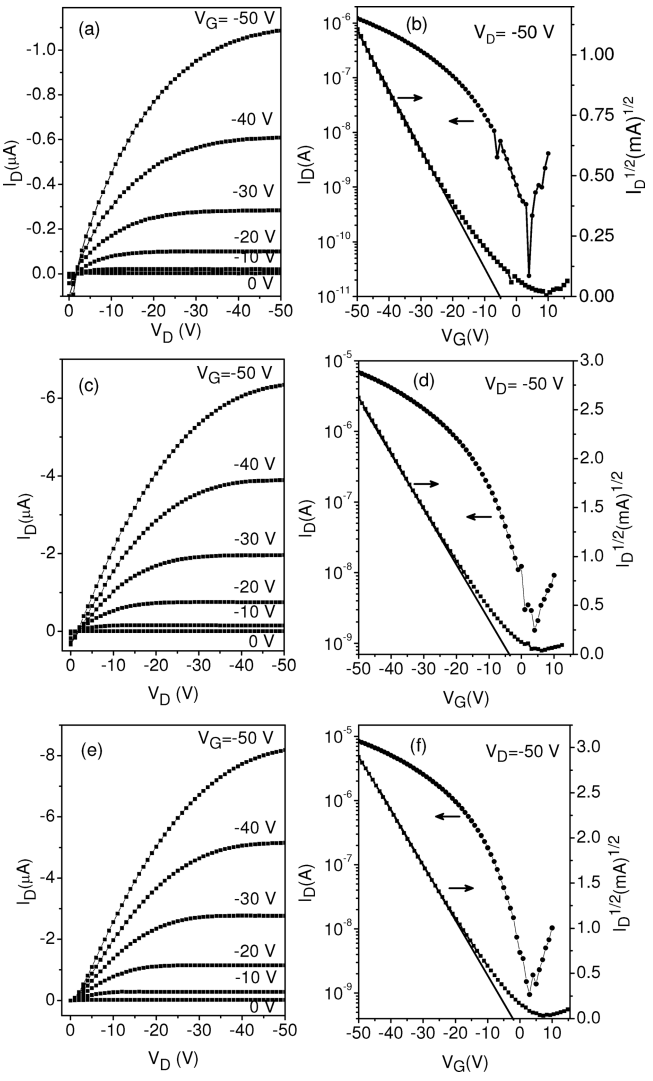

Figure 4. Typical output (a, c, e) and transfer (b, d, f) characteristics of OTFT devices of **P-bTC10** (a, b), **P-bTC12** (c, d), and **P-bTC16** (e, f). All the polymer films were spin-coated from chlorobenzene solutions and annealed for 20 min. The annealing temperatures are 180, 180, and 150 °C for **P-bTC10**, **P-bTC12**, and **P-bTC16**, respectively.

which exhibited OTFT mobilities close to 0.01 $cm^2/(V\ s)$.[31a] Our results indicate that large arenes can be promising building blocks

dx.doi.org/10.1021/ma2007249 |*Macromolecules* 2011, 44, 5178–5185

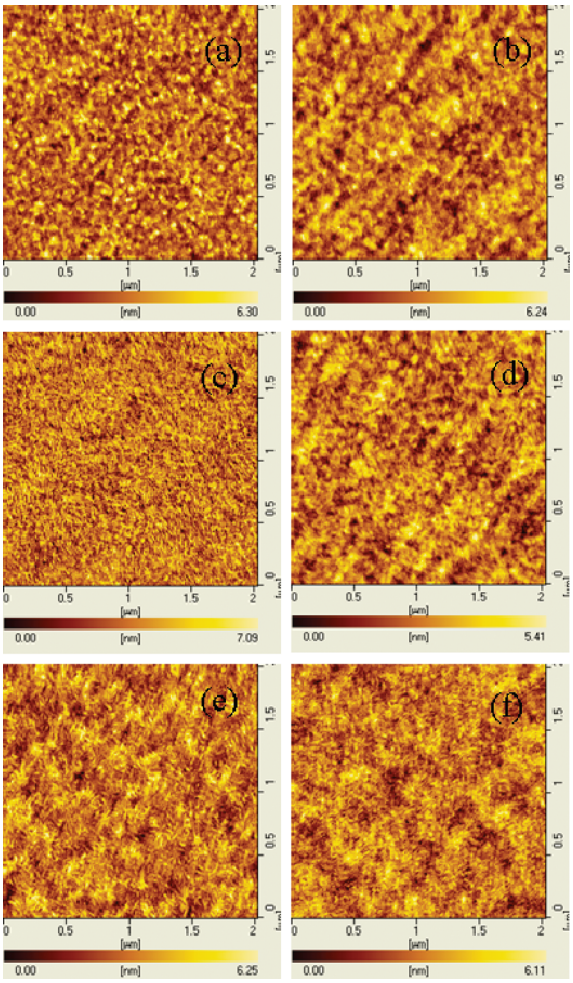

Figure 5. AFM height images of the pristine (a, c, e) and thermal annealed films (b, d, f) of **P-bTC10** (a, b), **P-bTC12** (c, d), and **P-bTC16** (e, f). The thermal annealing (20 min) was done in glovebox at 180 °C for **P-bTC10** and **P-bTC12** and 150 °C for **P-bTC16**. The films (~50 nm) were prepared by spin-casting chlorobenzene solutions on HMDS-treated Si/SiO_2 substrates.

for construction of high-mobility conjugated polymers via carefully tuning the chemical structures.

Thin Film Morphology. The morphology of polymer thin films on HMDS treated Si/SiO_2 substrates were studied by tapping mode atomic force microscopy (AFM) and thin film X-ray diffraction (XRD). Figure 6 shows AFM images of the polymer thin films before and after thermal annealing. All polymer films are uniform with root-mean-square roughness of 0.8−1.2 nm. **P-bTC10** was observed to show less ordered nanostructures. Films of **P-bTC12** and **P-bTC16** display rodlike features at nanometer scales. Moreover, the nanostructures of **P-bTC16** are more obvious than that of **P-bTC12**, indicating a higher order arrangement of polymer chains. This observation is consistent with the highest mobility of **P-bTC16**. Figure 6 shows XRD patterns of thin films of **P-bTC10**, **P-bTC12**, and **P-bTC16**. Only a diffraction peak (100) was observed for each polymer. The 2θ angles are at 3.80°, 3.48°, and 3.06° for **P-bTC10**, **P-bTC12**, and **P-bTC16**, respectively, corresponding to the *d*-spacing values of 23.2, 25.4, and 28.8 Å. This implies a lamellar layered structure which is oriented normal to the substrate. However, the order of the films is relatively low since

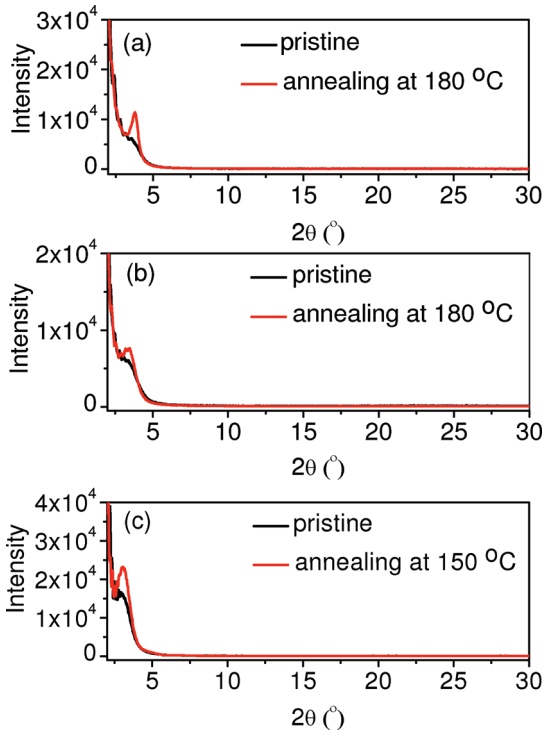

Figure 6. Thin film X-ray diffraction of **P-bTC10** (a), **P-bTC12** (b), and **P-bTC16** (c).

only the primary diffraction peaks were observed. Moreover, the *d*-spacing values are much larger than those of previously reported bithiophene/thienothiophene copolymers carrying similar alkyl chains.[11] This suggests that the side chains are less interdigitated or more loosely packed, which may be attributed to the large curvature of the polymer chains or different orientation of the alkyl chains.[18,32]

CONCLUSION

We have developed a novel S- and N-containing heteroarene, i.e., *N*-dodecyldithieno[2,3-*b*;7,6-*b*]carbazole, which contains five fused rings. Three alternating conjugated copolymers composed of the heteroarene and 4,4′-dialkyl-2,2′-bithiophenes were synthesized. The presence of a nitrogen atom in the heteroarene allows introducing more alkyl substituents in the polymer backbone. As a result, these polymers are highly soluble in various organic solvents. Solution spin-cast films of the polymers are characterized by a lamellar layered structure which is oriented normal to the substrate. Bottom gate, top contact OTFT devices were fabricated. It was found that mobility increased with the increase of the alkyl chain length in bithiophene units. **P-bTC16** exhibited the highest mobility up to 0.035 $cm^2/(V\ s)$, which is comparable to that of rr-P3HT reference devices. These findings strongly support the large heteroarenes as potential building blocks for high-mobility conjugated polymers.

EXPERIMENTAL SECTION

Measurement. ^1H and ^{13}C NMR spectra were recorded on a Bruker 300, 400, or 600 MHz spectrometer in $CDCl_3$ or $C_2D_2Cl_4$. Chemical shift was reported relative to an internal tetramethylsilane (TMS) standard for the measurements with $CDCl_3$ as solvent, while it was reported relative to the solvent signal for the measurements with

$C_2D_2Cl_4$ as solvent. Elemental analysis was performed on a VarioEL elemental analysis system. Matrix-assisted laser desorption ionization time-of-flight (MALDI-TOF) mass spectra were recorded on a Bruker/AutoflexIII Smartbean MALDI mass spectrometer with terthiophene as the matrix in reflection mode. TGA was carried out on a Perkin-Elmer TGA7 at a heating rate of 10 °C/min under nitrogen flow. DSC was performed on a Perkin-Elmer DSC 7 at a heating/cooling rate of 10/−10 °C/min under nitrogen flow. UV−vis absorption was recorded on a Shimadzu UV-3600 UV−vis−NIR spectrometer. GPC analysis was conducted on a Waters 510 system using polystyrene as standard and THF as eluent. The bandgap was calculated according to the onset absorption of UV−vis spectra ($E_g = 1240/\lambda_{onset}$ eV). Film CV measurements were performed on a HI660a electrochemical analyzer with a three-electrode cell at a scan rate of 100 mV s^{-1}. Bu_4NPF_6 (0.1 mol/L in acetonitrile for the scans in positive region and in DMF for the scans in negative region) was used as electrolyte. A glassy carbon electrode with a diameter of 10 mm, a Pt wire, and a saturated calomel electrode were used as the working, counter, and reference electrodes, respectively. To obtain electronic energy levels of the polymer films, the potential was calibrated against the ferrocene/ferrocenium (Fc/Fc^+). The highest occupied molecular orbital (HOMO) and the lowest unoccupied molecular orbital (LUMO) energy levels were estimated by the equations HOMO = $-(4.80 + E^{ox}_{onset})$ eV, LUMO = $-(4.80 - E^{re}_{onset})$ eV.[41] Thin-film X-ray diffraction (XRD) was recorded on a Bruker D8 Discover thin-film diffractometer with Cu Kα radiation (λ = 1.540 56 Å) operated at 40 keV and 40 mA. Atomic force microscopy (AFM) measurements were performed in tapping mode on a SPA400HV instrument with a SPI 3800 controller (Seiko Instruments).

Materials. THF, toluene, and ethyl ether (Et_2O) were distilled over sodium and benzophenone. Et_3N, DMF, and acetonitrile were distilled over CaH_2. *N*-Dodecyl-2,7-dibromocarbazole (**1**)[43] and 5,5′-dibromo-4,4′-dialkyl-2,2′-bithiophene[32] were synthesized according to literature procedures. Other reagents were obtained from commercial resources and used without further purification.

***N*-Dodecyl-2,7-dibromo-3,6-diiodocarbazole (2).** A mixture of the *N*-dodecyl-2,7-dibromocarbazole (**1**) (4.93 g, 10.0 mmol) and AcOH (100 mL) was heated to 80 °C, and then KI (4.43 g, 26.7 mmol) and KIO_3 (2.85 g, 13.3 mmol) were added in one portion. The mixture was stirred at 80 °C for 6 h and poured into water for extraction with CH_2Cl_2. The combined organic layers were washed with brine (2 × 100 mL) and dried over $MgSO_4$. After the solvent had been removed under reduced pressure, the residue was purified by recrystallization from alcohol to afford **2** as a white solid in a yield of 70.1% (5.20 g); mp: 109−110 °C. ^{1}H NMR (300 MHz, $CDCl_3$): δ (ppm) 8.46 (s, 2 H), 7.68 (s, 2 H), 4.14 (t, 2 H, J = 7.2 Hz), 1.79−1.83 (m, 2 H), 1.24−1.32 (m, 18 H), 0.88 (t, 3 H, J = 6.6 Hz). ^{13}C NMR (150 MHz, $CDCl_3$): δ (ppm) 141.1, 131.4, 126.7, 122.3, 113.0, 88.85, 43.48, 31.89, 29.57, 29.54, 29.52, 29.43, 29.31, 29.24, 28.61, 27.06, 22.68, 14.11. Anal. Calcd for $C_{24}H_{29}Br_2I_2N$ (%): C, 38.69; H, 3.92; N, 1.88. Found: C, 38.50; H, 3.80; N, 1.82.

***N*-Dodecyl-2,7-dibromo-3,6-di(trimethylsilylethynyl)carbazole (3).** Into a Schlenk flask charged with $Pd(PPh_3)_2Cl_2$ (10 mg, 0.014 mmol), CuI (54 mg, 0.028 mmol), and **2** (11.9 g, 16.0 mmol) were added Et_3N (80 mL) and THF (80 mL). After addition of trimethylsilylacetylene (3.20 g, 32.7 mmol) dropwise, the mixture was stirred at room temperature for 48 h. The resulting yellow suspension was diluted with ethyl acetate (300 mL). The organic layer was washed with saturated aqueous ammonium chloride (500 mL) and brine (2 × 200 mL). After the solvent had been removed, the residue was purified by column chromatography on silica gel with dichloromethane:petroleum ether = 1:4 (v/v) as eluent to afford **3** as colorless oil in a yield of 56.4% (6.18 g). ^{1}H NMR (300 MHz, $CDCl_3$): δ (ppm) 8.15 (s, 2 H), 7.57 (s, 2 H), 4.15 (t, 2 H, J = 7.2 Hz), 1.79−1.83 (m, 2 H), 1.24−1.32 (m, 18 H), 0.87 (t, 3 H, J = 6.7 Hz), 0.31 (s, 18 H). ^{13}C NMR (75 MHz, $CDCl_3$): δ (ppm) 140.9, 125.5, 123.5, 121.1, 116.3, 112.8, 103.9, 97.35, 43.49, 31.89, 29.57, 29.50, 29.44, 29.31, 29.23, 28.68, 27.06, 22.68, 14.13. Anal. Calcd for $C_{34}H_{47}Br_2NSi_2$(%): C, 59.55; H, 6.91; N, 2.04. Found: C, 59.57; H, 6.66; N, 1.69.

***N*-Dodecyldithieno[2,3-*b*;7,6-*b*]carbazole (4).** To the suspension of sodium sulfide nonahydrate (8.41 g, 35.0 mmol) in NMP (175 mL) was added **3** (6.00 g, 8.75 mmol) and then stirred at 190 °C for 12 h. After being poured into 200 mL of saturated aqueous ammonium chloride solution, the mixture was extracted with Et_2O (3 × 100 mL). The organic layer was washed with brine (3 × 100 mL), dried over $MgSO_4$, and evaporated under reduced pressure. The crude product was purified by column chromatography on silica gel with petroleum ether as eluent to afford **4** as a white solid in a yield of 67.9% (2.66 g); mp: 138−139 °C. ^{1}H NMR (300 MHz, $CDCl_3$): δ (ppm) 8.55 (s, 2 H), 7.79 (s, 2 H), 7.47 (d, 2 H, J = 5.7 Hz), 7.32 (d, 2 H, J = 5.7 Hz), 4.32 (t, 2 H, J = 7.5 Hz,) 1.90−1.95 (m, 2 H), 1.24−1.47 (m, 18 H), 0.86 (t, 3 H, J = 6.7 Hz,) 0.31(s, 18 H). ^{13}C NMR (150 MHz, $CDCl_3$): δ (ppm) 140.8, 139.0, 132.8, 123.8, 122.9, 122.5, 114.5, 100.7, 43.44, 31.90, 29.58, 29.52, 29.45, 29.38, 29.31, 28.33, 27.36, 22.67, 14.11. Anal. Calcd for $C_{28}H_{33}NS_2$(%): C, 75.12; H, 7.43; N, 3.13. Found: C, 74.95; H, 7.67; N, 2.95. MALDI-TOF: calcd for $C_{28}H_{33}NS_2$, 447.21; found, 447.2.

***N*-Dodecyl-3,8-bis(trimethylstannyl)dithieno[2,3-*b*;7,6-*b*]carbazole (5).** At −20 °C, into the solution of **4** (447 mg, 1.00 mmo1) in THF (10 mL) was added *n*-BuLi (0.84 mL, 2.1 mmol, 2.5 M in hexanes) via syringe. The mixture was maintained at this temperature for 30 min, warmed to room temperature for another 1 h, and then recooled to −20 °C. Trimethyltin chloride (409 mg, 2.05 mmol) was added at once. The mixture was stirred overnight at room temperature and poured into water for extraction with CH_2Cl_2 (3 × 70 mL). The combined organic layers were washed with aqueous KF and brine and dried over $MgSO_4$. After the solvent had been removed under reduced pressure, the residue was purified by recrystallization from hexane to afford **5** as a white solid in a yield of 85.0% (657 mg); mp: 174−175 °C. ^{1}H NMR (300 MHz, $CDCl_3$): δ (ppm) 8.52 (s, 2 H), 7.78 (s, 2 H), 7.53 (s, 2 H), 4.31 (t, 2 H, J = 7.20 Hz), 1.89−1.94 (m, 2 H), 1.23−1.42 (m, 18 H), 0.87 (t, 3 H, J = 6.7 Hz), 0.45 (s, 18 H). ^{13}C NMR (150 MHz, $CDCl_3$): δ (ppm) 143.4, 140.7, 136.3, 134.5, 132.0, 122.6, 113.5, 100.1, 43.39, 31.89, 29.57, 29.50, 29.45, 29.31, 28.28, 27.33, 22.67, 14.11. Anal. Calcd for $C_{34}H_{49}NS_2Sn_2$ (%): C, 52.81; H, 6.39; N, 1.81. Found: C, 52.61; H, 6.42; N, 1.30.

General Synthesis Procedure of Polymers (P-bTCn). A mixture of **5** (315 mg, 0.408 mol), 5,5′-dibromo-4,4′-dialkyl-2,2′-bithiophene (0.40 mol), tris(dibenzylideneacetone)dipalladium (Pd_2dba_3, 7.32 mg, 0.008 mmol), and tri-*o*-tolylphosphine ($P(o\text{-}Tol)_3$, 19.5 mg, 0.064 mmol) was degassed with argon, and then toluene (40 mL) was added. The mixture was further purged with argon for 10 min and heated to 120 °C for 48 h. Then 4-bromotoluene (28.0 mg, 0.163 mmol) was added, and the reaction was continued for another 12 h. The polymer was precipitated in methanol. The crude polymer was collected by filtration and then extracted on a Soxhlet's extractor with acetone, hexane, and chloroform in succession. The final product was obtained by precipitating the chloroform solution in methanol.

P-bTC10: red powders, 78.4% yield. ^{1}H NMR (400 MHz, $C_2D_2Cl_4$, 80 °C): δ (ppm) 8.46 (s, 2 H), 7.71 (s, 2 H), 7.46 (s, 2 H), 7.08 (s, 2 H), 4.30 (s, 2 H), 2.87 (s, 4 H), 1.95 (s, 2 H), 1.75 (s, 4 H), 1.28−1.45 (br, 46 H), 0.88 (s, 9 H). GPC: M_n = 19 500 g mol^{-1}, PDI = 2.37. Anal. Calcd for $C_{56}H_{77}NS_4$ (%): C, 75.36; H, 8.70; N, 1.57. Found: C, 75.27; H, 8.79; N, 1.60.

P-bTC12: red powders, 84.4% yield. ^{1}H NMR (400 MHz, $C_2D_2Cl_4$, 80 °C): δ (ppm) 8.46 (s, 2 H), 7.71 (s, 2 H), 7.48 (s, 2 H), 7.09 (s, 2 H), 4.30 (s, 2 H), 2.90 (s, 4 H), 1.97 (s, 2 H), 1.78 (s, 4 H), 1.29−1.46 (br, 54 H), 0.88 (s, 9 H). GPC: M_n = 18 600 g mol^{-1}, PDI = 2.14. Anal. Calcd for $C_{60}H_{85}NS_4$ (%): C, 75.97; H, 9.03; N, 1.48. Found: C, 75.94; H, 8.90; N, 1.41.

P-bTC16: orange red powders, 75.5% yield. ^{1}H NMR (400 MHz, $C_2D_2Cl_4$, 80 °C): δ (ppm) 8.47 (s, 2 H), 7.72 (s, 2 H), 7.49 (s, 2 H), 7.09 (s, 2 H), 4.31 (s, 2 H), 2.90 (s, 4 H), 1.97 (s, 2 H), 1.77 (s, 4 H), 1.27−1.44 (br, 70 H), 0.87 (s, 9 H). GPC: M_n = 21 700 g mol^{-1}, PDI = 1.91. Anal. Calcd for $C_{68}H_{101}NS_4$ (%): C, 76.99; H, 9.60; N, 1.32. Found: C, 76.38; H, 9.67; N, 1.32.

OFET Device Fabrication and Characterization. OFETs were fabricated in a top-contact configuration on heavily doped n-type Si wafers covered with 300 nm thick thermally grown SiO_2 (C_i = 10 nF cm^{-2}). The Si/SiO_2 substrates were carefully cleaned according to the literature procedure and then treated with a HMDS to form a self-assembled monolayer (SAM).[42] The polymer films were spin-coated from 6.5 mg/mL solution in chlorobenzene or toluene with 1000 rpm for 60 s, subsequently annealed at 150 or 180 °C for 20 min in the glovebox. Au drain and source electrodes (thickness 40 nm) were deposited in vacuum through a shadow mask. The channel length (L) and width (W) are 100 and 3000 μm, respectively. The electrical measurements were performed with two Keithley 236 source/measure units at room temperature in ambient atmosphere. The mobility data were collected from more than eight different devices.

■ ASSOCIATED CONTENT

Supporting Information. ^{1}H and ^{13}C NMR spectra of the intermediates and ^{1}H NMR spectra of the polymers. This material is available free of charge via the Internet at http://pubs.acs.org.

■ AUTHOR INFORMATION

Corresponding Author
*E-mail: yhgeng@ciac.jl.cn.

■ ACKNOWLEDGMENT

This work is supported by National Basic Research Program of China (973 Project, No. 2009CB623603) of Chinese Ministry of Science and Technology, NSFC (Nos. 20921061 and 50833004).

■ REFERENCES

(1) Allard, S.; Forster, M.; Souharce, B.; Thiem, H.; Scherf, U. *Angew. Chem., Int. Ed.* **2008**, *47*, 2–31.
(2) Zhang, L.; Di, C. A.; Yu, G.; Liu, Y. Q. *J. Mater. Chem.* **2010**, *20*, 7059–7073.
(3) Arias, A. C.; MacKenzie, J. D.; McCulloch, I.; Rivnay, J.; Salleo, A. *Chem. Rev.* **2010**, *110*, 3–24.
(4) Facchett, A. *Chem. Mater.* **2011**, *23*, 733–758.
(5) Ong, B. S.; Wu, Y.; Li, Y.; Liu, P.; Pan, H. *Chem.—Eur. J.* **2008**, *14*, 4766–4778.
(6) Osaka, I.; McCullough, R. D. *Acc. Chem. Res.* **2008**, *41*, 1202–1214.
(7) Sirringhaus, H.; Brown, P. J.; Friend, R. H.; Nielsen, M. M.; Bechgaard, K.; Langeveld-Voss, B. M. W.; Spiering, A. J. H.; Janssen, R. A. J.; Meijer, E. W.; Herwig, P.; de Leeuw, D. M. *Nature* **1999**, *401*, 685–688.
(8) Ong, B. S.; Wu, Y.; Liu, P.; Gardner, S. *J. Am. Chem. Soc.* **2004**, *126*, 3378–3379.
(9) Liu, P.; Wu, Y.; Pan, H.; Ong, B. S. *Macromolecules* **2010**, *43*, 6368–6373.
(10) Li, Y.; Wu, Y.; Liu, P.; Birau, M.; Pan, H.; Ong, B. S. *Adv. Mater.* **2006**, *18*, 3029–3032.
(11) McCulloch, I.; Heeney, M.; Bailey, C.; Genevicius, K.; MacDonald, I.; Shkunov, M.; Sparrowe, D.; Tierney, S.; Wagner, R.; Zhang, W.; Chabinyc, M. L.; Kline, R. J.; McGehee, M. D.; Toney, M. F. *Nature Mater.* **2006**, *5*, 328–333.
(12) McCulloch, I.; Heeney, M.; Chabinyc, M. L.; DeLongchamp, D.; Kline, R. J.; Cölle, M.; Duffy, W.; Fischer, D.; Gundlach, D.; Hamadani, B.; Hamilton, R.; Richter, L.; Salleo, A.; Shkunov, M.; Sparrowe, D.; Tierney, S.; Zhang, W. *Adv. Mater.* **2009**, *21*, 1091–1109.
(13) Li, J.; Qin, F.; Li, C. M.; Bao, Q.; Chan-Park, M. B.; Zhang, W.; Qin, J.; Ong, B. S. *Chem. Mater.* **2008**, *20*, 2057–2059.
(14) Liu, J.; Zhang, R.; Sauvé, G.; Kowalewski, T.; McCullough, R. D. *J. Am. Chem. Soc.* **2008**, *130*, 13167.
(15) Zhang, W.; Li, J.; Zou, L.; Zhang, B.; Qin, J. G.; Lu, Z. S.; Poon, Y. F.; Chan-Park, M. B.; Li, C. M. *Macromolecules* **2008**, *41*, 8953–8955.
(16) Pan, H; Li, Y.; Wu, Y.; Liu, P.; Ong, B. S.; Zhu, S.; Xu, G. *J. Am. Chem. Soc.* **2007**, *129*, 4112–4113.
(17) Rieger, R.; Beckmann, D.; Pisula, W.; Steffen, W.; Kastler, M.; Müllen, K. *Adv. Mater.* **2010**, *22*, 83–86.
(18) Rieger, R.; Beckmann, D.; Mavrinskiy, A.; Kastler, M.; Müllen, K. *Chem. Mater.* **2010**, *22*, 5314–5318.
(19) Osaka, I.; Sauvé, G.; Zhang, R.; Kowalewski, T.; McCullough, D. *Adv. Mater.* **2007**, *19*, 4160–4165.
(20) Osaka, I.; Takimiya, K.; McCullough, R. D. *Adv. Mater.* **2010**, *22*, 4993–4997.
(21) Liu, J.; Zhang, R.; Osaka, I.; Mishra, S.; Javier, A. E.; Smilgies, D.-M.; Kowalewski, T.; McCullough, D. *Adv. Funct. Mater.* **2009**, *19*, 3427–3434.
(22) Kim, D. H.; Lee, B. L.; Moon, H.; Kang, H. M.; Jeong, E. J.; Park, J.-Il; Han, K. M.; Lee, S.; Yoo, B. W.; Koo, B. W.; Kim, J. Y.; Lee, W. H.; Cho, K.; Becerril, H. A.; Bao, Z. N. *J. Am. Chem. Soc.* **2009**, *131*, 6124–6132.
(23) Yang, C.; Cho, S.; Chiechi, R. C.; Walker, W.; Coates, N. E.; Moses, D.; Heeger, A. J.; Wudl, F. *J. Am. Chem. Soc.* **2008**, *130*, 16524–16526.
(24) Yue, W.; Zhao, Y.; Tian, H. K.; Song, D.; Xie, Z. Y.; Yan, D. H.; Geng, Y. H.; Wang, F. S. *Macromolecules* **2009**, *42*, 6510–6518.
(25) Kelley, T. W.; Muyres, D. V.; Baude, P. F.; Jones, T. D. *Mater. Res. Soc. Symp. Proc.* **2003**, *771*, L6.5.1–L6.5.10.
(26) Izawa, T.; Miyazaki, E.; Takimiya, K. *Adv. Mater.* **2008**, *20*, 3388–3392.
(27) Yamamoto, T.; Takimiya, K. *J. Am. Chem. Soc.* **2007**, *129*, 2224–2225.
(28) Gao, P.; Beckmann, D.; Tsao, H. N.; Feng, X.; Enkelmann, V.; Baumgarten, M.; Pisula, W.; Müllen, K. *Adv. Mater.* **2009**, *21*, 213–216.
(29) Gao, J.; Li, R.; Li, L.; Meng, Q.; Jiang, H.; Li, H.; Hu, W. *Adv. Mater.* **2007**, *19*, 3008–3011.
(30) Okamoto, T.; Bao, Z. N. *J. Am. Chem. Soc.* **2007**, *129*, 10308–10309.
(31) (a) Jiang, Y.; Okamoto, T.; Becerril, H. A.; Hong, S.; Tang, M. L.; Mayer, A. C.; Parmer, J. E.; McGehee, M. D.; Bao, Z. N. *Macromolecules* **2010**, *43*, 6361–6367. (b) Okamoto, T.; Jiang, Y.; Qu, F.; Mayer, A. C.; Parmer, J. E.; McGehee, M. D.; Bao, Z. N. *Macromolecules* **2008**, *41*, 6977–6980.
(32) Fong, H. H.; Pozdin, V. A.; Amassian, A.; Malliaras, G. G.; Smilgies, D.-M.; He, M.; Gasper, S.; Zhang, F.; Sorensen, M. L. *J. Am. Chem. Soc.* **2008**, *130*, 13202–13203.
(33) He, M.; Li, J.; Sorensen, M. L.; Zhang, F.; Hancock, R. R.; Fong, H. H.; Pozdin, V. A.; Smilgies, D.-M.; Malliaras, G. G. *J. Am. Chem. Soc.* **2009**, *131*, 11930–11938.
(34) Osaka, I.; Abe, T.; Shinamura, S.; Miyazaki, E.; Takimiya, K. *J. Am. Chem. Soc.* **2010**, *132*, 5000–5001.
(35) Rieger, R.; Beckmann, D.; Pisula, W.; Kastler, M.; Müllen, K. *Macromolecules* **2010**, *43*, 6264–6267.
(36) Morin, J.-F.; Leclerc, M.; Adès, D; Siove, A. *Macromol. Rapid Commun.* **2005**, *26*, 761–778.
(37) Blouin, N; Leclerc, M. *Acc. Chem. Res.* **2008**, *41*, 1110–1119.
(38) Li, Y.; Wu, Y.; Ong, B. S. *Macromolecules* **2006**, *39*, 6521–6527.
(39) Zhang, Q.; Chen, J. S.; Cheng, Y. X.; Wang, L. X.; Ma, D. G.; Jing, X. B.; Wang, F. S. *J. Mater. Chem.* **2004**, *14*, 895–900.
(40) (a) Kashiki, T.; Shinamura, S.; Kohara, M.; Miyazaki, E.; Takimiya, K.; Ikeda, M.; Kuwabara, H. *Org. Lett.* **2009**, *11*, 2473–2475. (b) Shinamura, S.; Miyazaki, E.; Takimiya, K. *J. Org. Chem.* **2010**, *75*, 1228–1234.

(41) Bard, A. J.; Faulkner, L. A. *Electrochemical Methods — Fundamentals and Applications*; Wiley: New York, 1984.
(42) (a) Salleo, A; Chabinyc, M. L.; Yang, M. S.; Street, R. A. *Appl. Phys. Lett.* **2002**, *81*, 4383–4385. (b) Yoon, M.-H.; DiBenedetto, S. A.; Facchetti, A.; Marks, T. J. *J. Am. Chem. Soc.* **2005**, *127*, 1348–1349.
(43) Dierschke, F.; Grimsdale, A. C.; Müllen, K. *Synthesis* **2003**, *16*, 2470–2472.